

# RSC Sustainability

Accepted Manuscript

This article can be cited before page numbers have been issued, to do this please use: M. Karuppusamy, S. Palanisamy, S. Balakrishnamoorthi, A. R. Rajendran, S. P. Velmurugan, K. Sureshkumar, S. K. Ali, S. L. Sankar, K. Sundararajan, A. Alagarsamy and M. Belay, *RSC Sustainability*, 2026, DOI: 10.1039/D6SU00165C.



This is an Accepted Manuscript, which has been through the Royal Society of Chemistry peer review process and has been accepted for publication.

Accepted Manuscripts are published online shortly after acceptance, before technical editing, formatting and proof reading. Using this free service, authors can make their results available to the community, in citable form, before we publish the edited article. We will replace this Accepted Manuscript with the edited and formatted Advance Article as soon as it is available.

You can find more information about Accepted Manuscripts in the [Information for Authors](#).

Please note that technical editing may introduce minor changes to the text and/or graphics, which may alter content. The journal's standard [Terms & Conditions](#) and the [Ethical guidelines](#) still apply. In no event shall the Royal Society of Chemistry be held responsible for any errors or omissions in this Accepted Manuscript or any consequences arising from the use of any information it contains.

## Sustainability Spotlight

View Article Online  
DOI: 10.1039/D6SU00165C

This study demonstrates a sustainable materials strategy by combining natural fibers (milkweed and *Aristida hystrix*) with bio-waste peanut shell powder to develop high-performance epoxy composites. By optimizing fiber hybridization and utilizing agricultural waste as a functional filler, the work reduces reliance on synthetic reinforcements, enhances material efficiency, and promotes circular resource use—offering an eco-friendly pathway for lightweight structural applications.



# Mechanical, Morphological and Interfacial Characterization of Peanut Shell Powder Modified Milkweed–*Aristida hystrix* Hybrid Fiber Reinforced Epoxy Composites

Manickaraj Karuppusamy<sup>1</sup>, Sivasubramanian Palanisamy<sup>2\*</sup>, Silambarasan Balakrishnamoorthi<sup>3</sup>, Ashok Raj Rajendran<sup>4</sup>, Subbiah Parvathy Velmurugan<sup>5</sup>, Kumar Sureshkumar<sup>6</sup>, Syed Kashif Ali<sup>7,8</sup>, Subramanian Lakshmi Sankar<sup>9</sup>, Karthikayan Sundararajan<sup>2</sup>, Aravindhyan Alagarsamy<sup>10</sup>, Mezigebe Belay<sup>11\*</sup>

<sup>1</sup>Department of Mechanical Engineering, CMS College of Engineering and Technology, Coimbatore- 641032, Tamilnadu, India.

<sup>2</sup>Department of Mechanical Engineering, School of Engineering, Mohan Babu University, Tirupati - 517102, Andhra Pradesh, India.

<sup>3</sup>Department of Mechanical Engineering, Sir Issac Newton College of Engineering and Technology, Nagapattinam -611102, Tamil Nadu, India

<sup>4</sup>Department of Mechanical Engineering, J.J. College of Engineering and Technology, Trichy, Tamilnadu – 620009, India.

<sup>5</sup>Department of Electronics and Communication Engineering, Kalasalingam Academy of Research and Education, Krishnankoil - 626126, Srivilliputhur, Tamilnadu, India.

<sup>6</sup>Department of Electronics and Communication Engineering, Koneru Lakshmaiah Education Foundation, Vaddeswaram-522501, Andhra Pradesh, India.

<sup>7</sup>Department of Physical Sciences, Chemistry Division, College of Science, Jazan University, P.O. Box. 114, Jazan 45142, Kingdom of Saudi Arabia.

<sup>8</sup>Engineering and Technology Research Center, Jazan University, P.O. Box. 114, Jazan 45142, Kingdom of Saudi Arabia.

<sup>9</sup>Department of Mechanical Engineering, Sathyabama Institute of Science and Technology, Chennai, Tamilnadu, India.

<sup>10</sup>Center for Flexible Electronics, Department of Electronics and Communication Engineering, Koneru Lakshmaiah Education Foundation, Vaddeswaram-522501, Andhra Pradesh, India.

<sup>11</sup>Department of Metallurgical and Materials Engineering, College of Engineering, Ethiopian Defence University, Bishoftu, 1041, Ethiopia.

\*Corresponding authors: [sivaresearch948@gmail.com](mailto:sivaresearch948@gmail.com); [mezgebubelay@etdu.edu.et](mailto:mezgebubelay@etdu.edu.et)



## Abstract

The present study investigates the effect of fiber hybridization and peanut shell powder filler incorporation on the mechanical and interfacial performance of milkweed and *Aristida hystrix* fiber reinforced epoxy composites. A series of hybrid composites were fabricated by maintaining a constant epoxy content (60 wt%) and peanut shell powder filler content (10 wt%), while systematically varying the weight fractions of milkweed and *Aristida hystrix* fibers. Mechanical characterization was carried out through tensile, flexural, impact, hardness, interlaminar shear strength (ILSS), tensile modulus, and flexural modulus tests. The results indicate a pronounced improvement in mechanical properties with increasing hybridization, achieving optimum performance at an equal fiber distribution (H3: 15 wt% milkweed + 15 wt% *Aristida hystrix*). The H3 composite exhibited the highest tensile strength (61 MPa), flexural strength (86 MPa), impact strength (10.2 J), hardness (83 Shore D), ILSS (12.1 MPa), tensile modulus (3.5 GPa), and flexural modulus (4.1 GPa). Scanning electron microscopy (SEM) analysis of fractured surfaces revealed improved fiber–matrix interfacial adhesion, reduced fiber pull-out, and uniform filler dispersion in the optimized hybrid composites, corroborating the enhanced mechanical performance. In contrast, the unfilled composite exhibited interfacial debonding and void formation, leading to inferior properties. The combined use of fiber hybridization and bio-based peanut shell powder filler is thus demonstrated as an effective approach for developing sustainable, high-performance epoxy composites suitable for lightweight structural applications.

**Keywords:** Milkweed fiber; *Aristida hystrix* fiber; Peanut shell powder; Hybrid composites; Mechanical performance; SEM analysis

## 1. Introduction

Growing environmental concerns, depletion of fossil-based resources, and increasingly stringent regulations on carbon emissions have significantly accelerated research into sustainable engineering materials<sup>1</sup>. In this context, natural fiber reinforced polymer composites have emerged as a promising alternative to conventional synthetic fiber composites due to their low density, renewability, biodegradability, cost-effectiveness, and reduced environmental footprint. These advantages make natural fiber composites attractive for applications in automotive components, building materials, consumer products, and lightweight structural panels.



Additionally, natural fibers require less energy for processing and offer improved end-of-life disposal options compared to glass or carbon fibers<sup>2–4</sup>.

Despite these advantages, composites reinforced with a single type of natural fiber often exhibit several inherent limitations. Poor fiber–matrix interfacial bonding, high moisture absorption, variability in fiber morphology, and inconsistent mechanical performance remain critical challenges that restrict their widespread structural application<sup>5,6</sup>. The hydrophilic nature of lignocellulosic fibers leads to weak adhesion with hydrophobic polymer matrices, resulting in inefficient stress transfer and premature failure under mechanical loading. Furthermore, single-fiber systems may not simultaneously satisfy the competing requirements of strength, stiffness, toughness, and impact resistance<sup>7–9</sup>.

To overcome these limitations, fiber hybridization has been widely adopted as an effective strategy. Fiber hybridization involves the incorporation of two or more fibers with distinct physical and mechanical characteristics within a single polymer matrix, enabling the synergistic combination of their individual advantages<sup>10–12</sup>. Hybrid composites often demonstrate improved mechanical performance, damage tolerance, and reliability compared to mono-fiber composites. The hybridization concept is particularly beneficial in natural fiber composites, where one fiber can compensate for the deficiencies of another, resulting in balanced and optimized performance<sup>13,14</sup>.

Milkweed fiber has gained attention in recent years due to its unique hollow structure, ultra-low density, and excellent energy absorption capability. The hollow lumen present within milkweed fibers contributes to reduced composite density and enhanced damping and impact resistance<sup>15</sup>. These characteristics make milkweed fiber attractive for lightweight and insulation-oriented applications<sup>16–18</sup>. However, milkweed fiber exhibits relatively low tensile strength and stiffness, which limits its load-bearing capability in structural applications. The weak mechanical strength of milkweed fiber necessitates hybridization with a stiffer reinforcement to enhance the overall composite performance<sup>19–21</sup>.

In contrast, *Aristida hystrix*, commonly known as porcupine grass, is a lesser-explored natural grass fiber belonging to the Poaceae family. Grass fibers such as *Aristida hystrix* are



characterized by higher cellulose content, relatively low microfibril angle, and improved stiffness compared to many seed or bast fibers<sup>22,23</sup>. These attributes contribute to better tensile and flexural performance when used as reinforcement in polymer matrices. Despite its promising characteristics, *Aristida hystrix* fiber remains underutilized in composite research, particularly in hybrid configurations<sup>24–26</sup>. The combination of milkweed fiber and *Aristida hystrix* fiber is therefore expected to produce a synergistic effect, where the lightweight and energy-absorbing nature of milkweed fiber complements the stiffness and strength of the grass fiber<sup>27,28</sup>.

Beyond fiber hybridization, recent research has increasingly focused on the incorporation of bio-based fillers derived from agricultural waste as a sustainable approach to further enhance composite performance. Agricultural residues such as nut shells, fruit shells, husks, and sawdust are generated in large quantities worldwide and often remain underutilized or disposed of through environmentally harmful practices<sup>29,30</sup>. Converting these wastes into functional fillers not only adds value to biomass resources but also improves the sustainability of composite materials<sup>31</sup>.

Peanut shell powder is abundant agro-waste material rich in cellulose, hemicellulose, and lignin. When finely processed and incorporated into polymer composites, peanut shell powder can act as a micro-scale reinforcement and interfacial modifier. The presence of rigid lignocellulosic particles enhances stress transfer between fibers and matrix, reduces micro-voids, and restricts crack propagation under mechanical loading<sup>32–34</sup>. Moreover, the filler particles improve composite compactness and surface hardness while contributing to waste valorization and cost reduction. However, excessive filler content may lead to agglomeration and stress concentration, making controlled incorporation essential<sup>35</sup>.

Although several studies have reported the effects of fiber hybridization or bio-based filler addition individually, very limited research has examined the combined influence of milkweed fiber, rare grass fibers such as *Aristida hystrix*, and peanut shell powder filler within an epoxy matrix<sup>36–38</sup>. The interactive effects between lightweight hollow fibers, stiff grass fibers, and particulate bio-fillers on mechanical strength, stiffness, interlaminar behavior, and fracture morphology remain insufficiently explored. Understanding these interactions is crucial for designing high-performance, sustainable composites with optimized properties<sup>39</sup>.



This study presents a novel hybrid composite system incorporating milkweed fiber, *Aristida hystrix* fiber, and peanut shell powder as a bio-based filler. The combined effects of fiber hybridization and filler addition are systematically investigated to optimize mechanical and interfacial properties. A controlled compositional design is employed to identify an optimal balance between strength, stiffness, and toughness. Microstructural analysis is further utilized to establish structure–property relationships. The work contributes to the development of sustainable, high-performance composites using underutilized natural resources.

Thus, the current investigation attempts to systematically analyze and understand the influence of fiber hybridization and peanut shell powder addition on the mechanical and interfacial properties of epoxy matrix composites reinforced by milkweed and *Aristida hystrix* fibers<sup>40</sup>. Through a controlled experiment with a fixed quantity of epoxy and filler materials and varying amounts of fibers based upon their weights, there is a hope to discern a composite scheme that offers maximum tensile strength, flexural strength, impact strength, hardness value, and interlaminar shear strength properties<sup>41,42</sup>. Moreover, scanning electron microanalysis is used for scanning electron microscopic analysis for understanding and exploring microstructures characterized by mechanical properties<sup>42</sup>. Results of this investigation would provide valuable inputs for making lightweight yet strong and eco-friendly composites for various engineering applications.

### 3. Materials and Methods

#### 3.1 Materials

Milkweed fiber and *Aristida hystrix* fiber were used as the primary and secondary reinforcements, respectively. Both fibers were procured from local markets in and around the Coimbatore region, Tamil Nadu, India. The fibers were selected based on their availability, sustainability, and potential for reinforcement in polymer composites. Prior to composite fabrication, the fibers were cleaned to remove surface impurities and dried under ambient conditions to eliminate moisture content<sup>43</sup>. The figure 1 and 3 shows the milkweed and *Aristida hystrix* plant, figure 2 and 4 shows the milkweed and *Aristida hystrix* fiber.





Figure 1 Milkweed plant



Figure 2 Milkweed fiber



Figure 3 Aristida hystrix plant



Figure 4 Aristida hystrix fiber

Epoxy resin was used as the matrix material based on its high mechanical strength, dimensional stability, as well as adhesive properties with natural fibers. The epoxy resin material system was procured from Covai Seenu Company, Coimbatore, India, with its corresponding hardening agent compatible with the material. This resin-hardening agent mixture was chosen for its ability to be used for compression molding and natural fiber composite material preparation<sup>44</sup>.

Peanut shell powder (figure 6) was used as a bio-filler material. The peanut shells (figure 5) were extracted from local agricultural markets in and around Coimbatore and ground to fine powder mechanically<sup>45</sup>. The powder used as a filler material was sieved to ensure uniform particle size before mixing with the epoxy matrix<sup>46</sup>. The adoption of peanut shell powder not only increases composite material properties but also helps utilize agricultural wastes.





Figure 5 Peanut shell



Figure 6 Peanut shell powders

### 3.2 Composite Formulation

A total of six composite formulations (H0 to H5) were prepared. In all other filler combinations (H0 to H4), the weight percentage of epoxy resin was kept at 60 wt%, and peanut shell powder weight percentage as a filler was held constant at 10 wt%<sup>24,47</sup>. The last 30 wt% was a combination of milkweed and *Ariystdia hystrix* fibers. Composite H5 was prepared without any filler added to it so that it can act as a reference specimen<sup>48</sup>. The laminate compositions can be seen in Table 1.

Table 1 composite designations

Composite Code	Milkweed Fiber (wt%)	<i>Ariystdia hystrix</i> Fiber (wt%)	Peanut Shell Powder Filler	Epoxy Resin
H0	30	0	10	60
H1	25	5	10	60
H2	20	10	10	60
H3	15	15	10	60
H4	10	20	10	60
H5 (without filler)	30	30	0	60



### 3.3 Fabrication Process

The composites were fabricated using a hand lay-up technique followed by compression moulding to ensure effective consolidation and reduced void content. The epoxy resin and curing agent were mixed in the manufacturer-recommended ratio of 10:1 by weight and mechanically stirred at 500 rpm for 10 min to obtain a homogeneous mixture. Peanut shell powder (10 wt%) was then gradually incorporated into the resin system and further stirred for 15 min to ensure uniform dispersion and to minimize particle agglomeration [40]. Prior to fabrication, the milkweed and *Aristida hystrix* fibers were oven-dried at 80 °C for 24 h to remove moisture.

The dried fibers, arranged according to the required weight fractions, were uniformly placed in a pre-cleaned steel mould cavity with dimensions of 300 mm × 300 mm × 4 mm. The filler-loaded epoxy mixture was poured into the mould to ensure complete fiber impregnation. The mould was then closed and subjected to compression moulding using a hydraulic press at a pressure of 5 MPa and a temperature of 100 °C for 60 min to achieve proper curing and consolidation. To further enhance cross-linking, post-curing was carried out at 80 °C for 2 h in a hot air oven [41].

After curing, the mould was allowed to cool gradually to room temperature under pressure to minimize residual stresses before demoulding. The fabricated laminates were then trimmed and machined into test specimens as per relevant ASTM standards [42]. All specimens were prepared with dimensional accuracy using a diamond cutter to ensure consistency and repeatability of results.





Figure 7 sample composite plate

#### 4.0 Composite Testing

The fabricated milkweed–*Aristida hystrix* fiber-reinforced epoxy composites were subjected to comprehensive mechanical, interfacial, physical, and morphological characterization. All tests were conducted at room temperature under standard laboratory conditions, and the results are reported as the mean value of three specimens for each property to ensure improved repeatability and accuracy [43].

##### 4.1 Tensile Testing

Tensile strength, tensile modulus, and stress–strain relationship were assessed based on the ASTM D638 standard. Dog-bone shaped specimens were extracted from the laminates made of the composites, as specified in the standard size. The tensile test was done using the Universal Testing Machine, and the machine was operated at a fixed cross-head speed <sup>49</sup>. The values of the tensile strength were determined based on the maximum load at the point of breakage, and the values of the tensile modulus were determined based on the initial linear portion of the stress–strain diagram.



## 4.2 Flexural Testing

Flexural strength and flexural modulus were measured by a three-point bending test according to ASTM D790. Rectangular samples were measured under a specified span-to-depth ratio. The test demonstrates the bending strength of the composites, offering information on the rigidity and bearing strength in bending deformation. The value for the flexural modulus was obtained graphically from the load vs. sample deflection curve within the linear region <sup>50</sup>.

## 4.3 Impact Testing

The impact resistance was determined by the ASTM D256 standard using the Izod test impact method. The dimensions of the notched specimens of the composites tested for the energy of absorption during fracture were the standard dimensions of the test. The impact resistance of the composites depends on the absorption of the energy of the impact <sup>51</sup>.

## 4.4 Hardness Testing

The surface hardness of the composite materials was tested using the Shore D hardness test based on the ASTM D2240 standards. The test results are the average value of hardness measured at various points on the sample tested. The hardness test gives information on the resistance of the material to indentation and its stiffness <sup>52</sup>.

## 4.5 Interlaminar Shear Strength (ILSS) Testing

Interlaminar shear strength was determined using the short-beam shear test as per ASTM D2344. The test was conducted to evaluate fiber–matrix interfacial bonding and resistance to delamination under shear loading. ILSS was calculated based on the maximum load sustained by the specimen before failure <sup>53</sup>.

## 4.6 Morphological Analysis (SEM)

Scanning electron microscopy (SEM) was employed to analyze the fracture surfaces of selected tensile and impact-tested specimens. The analysis focused on fiber–matrix adhesion, filler dispersion, fiber pull-out, voids, and crack propagation mechanisms. The observed



microstructural features were correlated with the mechanical and interlaminar performance of the composites<sup>51</sup>.

## 5. Results and Discussion

### 5.1 Tensile Strength Analysis

The tensile strength of the milkweed–Aristida hystrix fibre reinforced epoxy composites is depicted in figure 8. A distinct and methodical variation in tensile strength is noted with alterations in fibre hybridisation and filler integration. The tensile strength values span from 38 MPa to 61 MPa, highlighting the considerable impact of fibre composition and interfacial integrity on load-bearing performance<sup>54</sup>. The composite H0, reinforced exclusively with milkweed fibre alongside peanut shell powder, demonstrated the lowest tensile strength recorded at 38 MPa. While milkweed fibre offers lightweight properties, its hollow structure and lower cellulose content restrict its ability to bear tensile loads. During tensile loading, the transfer of stress from the epoxy matrix to the milkweed fibres is not as effective, resulting in premature fibre deformation and cracking of the matrix. The restricted stiffness of milkweed fibre limits its capacity to prevent crack initiation, leading to early failure<sup>55–57</sup>. The introduction of Aristida hystrix fibre demonstrates a significant enhancement in tensile strength. Sample H1, which includes 25 wt% milkweed fibre and 5 wt% Aristida hystrix fibre, demonstrated a tensile strength of 45 MPa. The incorporation of grass fibre increased the stiffness of the composite and enhanced stress transfer efficiency, attributed to its elevated cellulose content and comparatively lower microfibril angle. The effect of hybridisation minimises stress concentration in the epoxy matrix and postpones the progression of cracks. An additional rise in the fibre content of Aristida hystrix in H2 (20 wt% milkweed + 10 wt% Aristida hystrix) led to a tensile strength of 53 MPa. In this composition, the effectiveness of the grass fibre in reinforcing the structure is increasingly evident, leading to enhanced load distribution between the two fibres. The inclusion of peanut shell powder filler significantly improves tensile performance by effectively filling micro-voids at the fiber-matrix interface and limiting interfacial debonding under load conditions. The filler particles serve as effective stress-transfer bridges, enhancing the continuity of the load path. The H3 composite demonstrated a maximum tensile strength of 61 MPa, incorporating equal amounts of milkweed and Aristida hystrix fibres, each constituting 15 wt% of the composite. This optimal



hybrid configuration demonstrates a significant synergistic effect, as the lightweight and energy-absorbing properties of milkweed fibre enhance the stiffness and strength of *Aristida hystrix* fibre. The even distribution of the fibres throughout the epoxy matrix facilitates efficient stress distribution and reduces localised stress concentrations. Furthermore, the inclusion of peanut shell powder as a filler enhances interfacial adhesion and minimises void content, which in turn improves the efficiency of stress transfer and postpones fibre pull-out<sup>58</sup>. In addition to the optimal hybrid ratio, sample H4 shows a minor decrease in tensile strength, recorded at 57 MPa. The elevated content of *Aristida hystrix* fibre contributes to enhanced stiffness; however, an overabundance of fibre can result in agglomeration, uneven dispersion, and inadequate wetting of the matrix. The presence of these factors leads to interfacial defects and localised stress concentration sites, adversely impacting tensile performance. The unfilled composite H5, while possessing a greater total fibre content, demonstrated a reduced tensile strength of 49 MPa in comparison to the optimised hybrid composite. The lack of peanut shell powder filler results in a higher number of micro-voids and a reduction in the strength of the fiber–matrix interfacial bonding, which facilitates fibre pull-out and matrix cracking when subjected to tensile loading. This finding underscores the essential contribution of integrating bio-based fillers to enhance interfacial integrity and overall tensile performance. The tensile strength results indicate that the combination of controlled fibre hybridisation and the incorporation of bio-based peanut shell powder filler significantly improves the tensile behaviour of epoxy composites<sup>59</sup>. The balanced hybrid configuration (H3) offers the highest efficiency in stress transfer and optimal interfacial bonding, positioning it as the most promising formulation for lightweight structural applications.



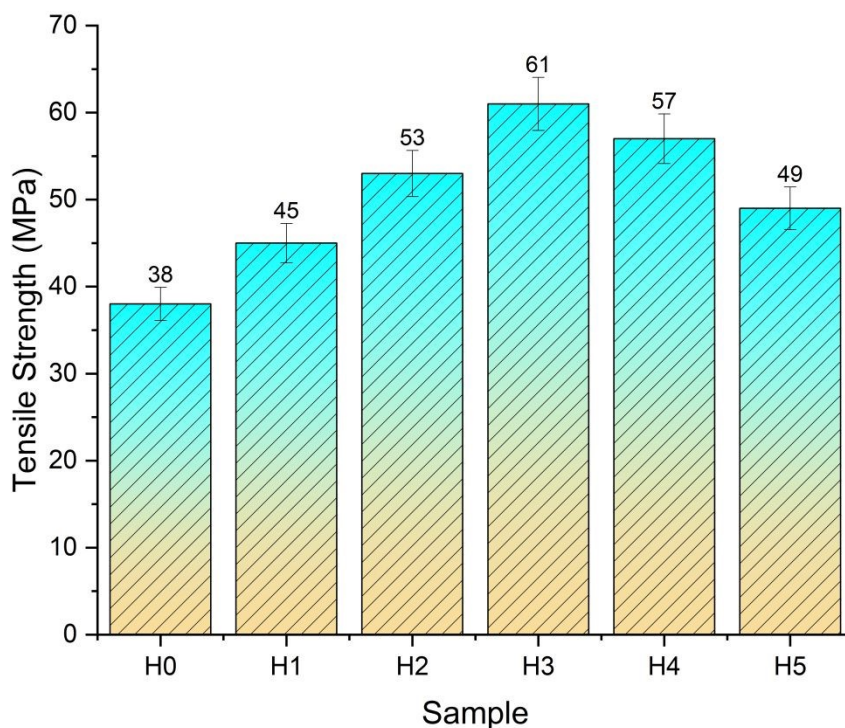


Figure 8 Tensile strength

## 5.2 Tensile Modulus Analysis

The tensile modulus of the milkweed–*Aristida hystrix* fiber-reinforced epoxy composites is depicted in figure 9. The findings indicate a gradual improvement in stiffness as fibre hybridisation increases, with a minor decrease observed at elevated grass fibre content. The tensile modulus values span from 2.4 to 3.5 GPa, effectively illustrating how fibre type, distribution, and interfacial characteristics impact the elastic behaviour of the composites<sup>60</sup>. The sample H0 exhibited the lowest tensile modulus at 2.4 GPa, featuring milkweed fibre as the exclusive reinforcement alongside peanut shell powder. The comparatively low stiffness of milkweed fibre can be explained by its hollow lumen structure and reduced cellulose content, which restricts its ability to resist elastic deformation when subjected to tensile loading. The addition of peanut shell powder enhances interfacial compactness; however, it is primarily the inherent stiffness of the reinforcing fibre that dictates the elastic behaviour at low strain levels<sup>61</sup>.



The introduction of *Aristida hystrix* fibre leads to a significant enhancement in tensile modulus. Sample H1 demonstrated a tensile modulus of 2.7 GPa, indicating the influence of the grass fiber's elevated cellulose content and reduced microfibril angle, which improves stiffness and limit elastic deformation. The hybridisation enhances the transfer of stress from the epoxy matrix to the fibres, leading to a more rigid composite response. Sample H2 demonstrates a notable enhancement in tensile modulus, achieving a value of 3.1 GPa. In this composition, the higher percentage of *Aristida hystrix* fibre notably improves load distribution within the composite. The consistent distribution of fibres along with the micro-filling properties of peanut shell powder minimises interfacial slippage, which in turn enhances resistance to elastic strain. This suggests a strong interaction between the fibre and matrix in the early linear phase of the stress-strain curve. The H3 composite, which includes equal proportions of milkweed and *Aristida hystrix* fibres, achieved an impressive tensile modulus of 3.5 GPa. This balanced hybrid configuration enhances fibre packing and ensures uniform stress distribution, resulting in improved elastic stiffness. The interaction between the lightweight milkweed fibre and the stiff grass fibre, along with improved interfacial adhesion from the inclusion of peanut shell powder, leads to increased resistance to elastic deformation. The findings demonstrate that H3 showcases the most effective mechanism for stress transfer within the elastic loading phase. A minor decrease in tensile modulus to 3.2 GPa is noted for sample H4. The elevated levels of *Aristida hystrix* fibre enhance stiffness; however, an overabundance of fibre can cause inadequate wetting and fibre clumping, resulting in interfacial flaws. The presence of these defects diminishes the effective load-bearing capacity of the fibres and constrains any potential improvements in modulus. The unfilled composite H5 demonstrated a tensile modulus of 2.5 GPa, which is less than that of the hybrid composites containing fillers. The lack of peanut shell powder results in heightened interfacial discontinuities and micro-voids, which diminishes fiber-matrix adhesion and elastic stiffness. This observation underscores the essential function of integrating bio-based fillers to enhance composite stiffness through improved interfacial integrity<sup>62</sup>. The tensile modulus results clearly indicate that the strategic hybridisation of fibres, along with the inclusion of peanut shell powder filler, markedly improves the elastic stiffness of epoxy composites. The optimised hybrid composite (H3) exhibits exceptional resistance to elastic deformation, rendering it ideal for applications that demand enhanced rigidity and dimensional stability<sup>63</sup>.



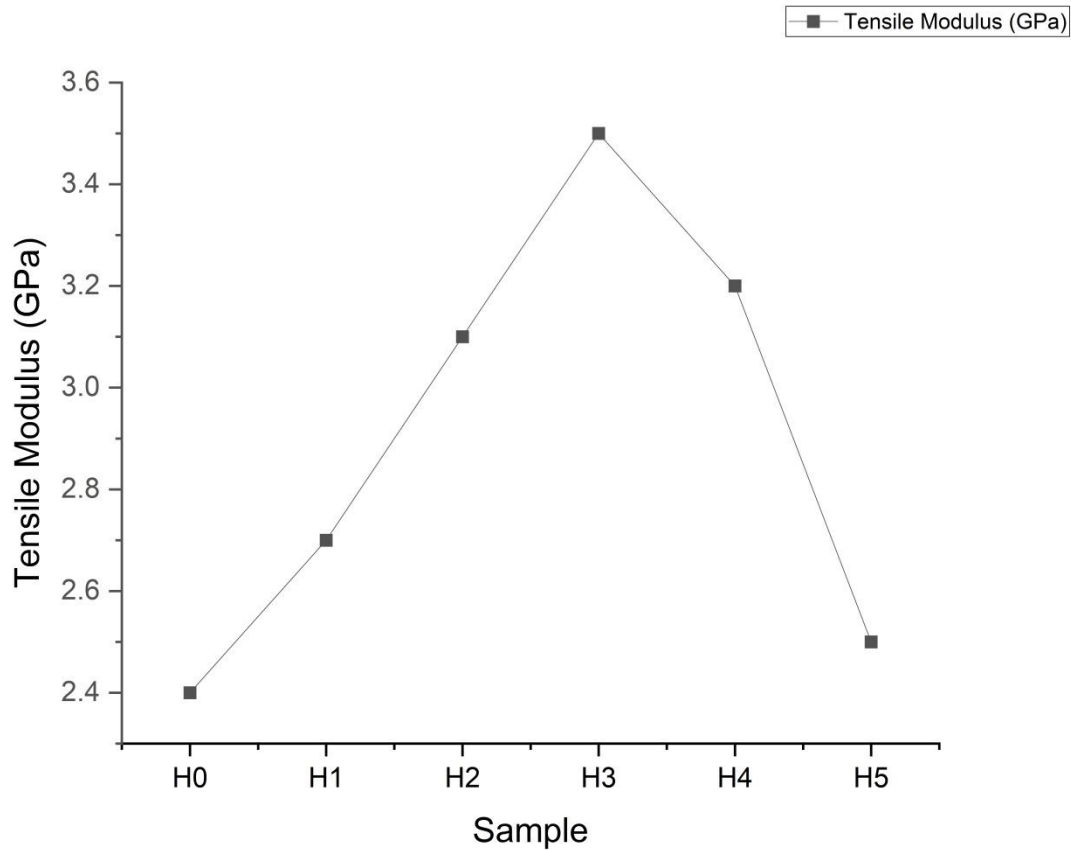


Figure 9 Tensile modulus

### 5.3 Tensile Stress–Strain Behavior

The tensile stress–strain behavior of the milkweed–*Aristida hystrix* fiber reinforced epoxy composites shows a clear dependence on fiber hybridization and peanut shell powder filler incorporation as shown in figure 10. All composites initially exhibit a linear elastic response up to about 1% strain, indicating effective elastic load transfer between the fibers and epoxy matrix. In this region, sample H0 shows the lowest slope, corresponding to its lower tensile modulus due to the dominance of milkweed fiber. In contrast, hybrid composites, particularly H2 and H3, display steeper slopes, confirming enhanced stiffness resulting from the higher content of *Aristida hystrix* fiber and improved interfacial bonding facilitated by the filler<sup>64</sup>. Beyond the elastic region, the stress–strain curves gradually become nonlinear as matrix yielding, fiber–matrix debonding, and microcrack initiation begin to occur. Sample H3 consistently records the



highest stress levels throughout this region, reaching a peak tensile stress of 62 MPa at approximately 2.5% strain. This superior performance is attributed to the optimized hybrid fiber ratio and uniform dispersion of peanut shell powder, which enhance stress redistribution and delay damage initiation. Samples H1 and H2 also show progressive improvement in stress-bearing capacity compared to H0, reflecting the positive synergistic effect of fiber hybridization<sup>65</sup>. After reaching the maximum stress, different failure behaviors are observed among the composites. Sample H3 sustains high stress over a wider strain range, extending up to about 5% strain, indicating improved ductility and damage tolerance. The gradual decline in stress beyond the peak suggests controlled failure dominated by fiber pull-out and crack deflection rather than sudden catastrophic fracture. Sample H4, although exhibiting relatively high tensile strength, shows an earlier post-peak stress reduction, likely due to fiber agglomeration and resin-deficient regions at higher *Aristida hystrix* fiber loading. Sample H2 maintains a balanced combination of strength and ductility, with sustained stress up to around 4% strain, highlighting effective stress transfer and fiber–matrix interaction. In contrast, sample H0 fails at lower strain with minimal post-peak deformation, indicating brittle behavior governed by matrix cracking and weak interfacial adhesion. Similarly, sample H5, which lacks peanut shell powder filler, exhibits reduced peak stress and earlier failure, emphasizing the critical role of filler particles in reinforcing the interfacial region and restricting crack propagation. Overall, the stress–strain behavior clearly demonstrates that the combined effect of fiber hybridization and bio-based filler incorporation significantly enhances tensile stiffness, strength, and failure strain. The optimized hybrid composite (H3) achieves the best balance between stiffness and ductility, making it a promising candidate for lightweight and sustainable structural applications<sup>66</sup>.



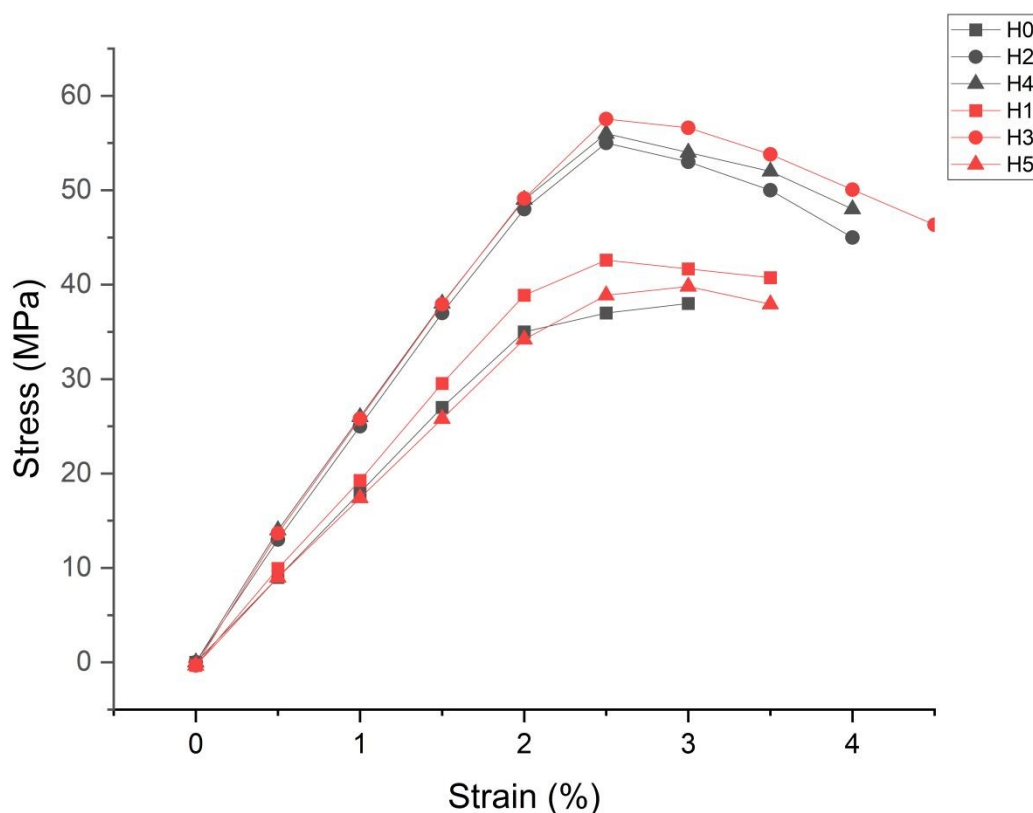


Figure 10 stress vs strain curve for tensile strength

#### 5.4 Flexural Strength Analysis

The flexural strength of the epoxy composites reinforced with milkweed–*Aristida hystrix* fibres is depicted in figure 11. The findings indicate a consistent enhancement in flexural strength as fibre hybridisation increases, with a slight reduction observed at elevated grass fibre content. The flexural strength values vary between 62 MPa and 86 MPa, underscoring the significant impact of fibre type, distribution, and interfacial integrity on bending performance. Sample H0, primarily reinforced with milkweed fibre alongside peanut shell powder, demonstrated the lowest flexural strength at 62 MPa. While milkweed fibre plays a role in decreasing density and enhancing energy absorption, its hollow architecture and relatively lower stiffness restrict its ability to withstand bending-induced stresses. Under flexural loading, tensile and compressive stresses are present on opposing surfaces of the specimen, and the limited stiffness of milkweed fibre diminishes its capacity to withstand deformation and the onset of cracks <sup>6,67</sup>. The addition



of *Aristida hystrix* fibre led to a significant improvement in flexural strength. Sample H1 demonstrated an increase to 69 MPa, reflecting enhanced resistance to bending attributed to the elevated stiffness and cellulose content of the grass fibre. The hybrid fibre system enhances load distribution among the fibres and the epoxy matrix, minimising deformation influenced by the matrix during flexural loading. Sample H2 shows notable enhancement, demonstrating a flexural strength of 78 MPa. The hybrid configuration at this fibre ratio offers improved stress distribution throughout the laminate thickness. The peanut shell powder filler is crucial as it fills micro-voids and enhances the fiber–matrix interface, which in turn limits crack propagation when subjected to bending loads. This results in enhanced load transfer efficiency and a postponement of failure. The sample H3 demonstrated the highest flexural strength at 86 MPa, incorporating equal proportions of milkweed and *Aristida hystrix* fibres. This balanced hybrid system demonstrates a significant synergistic effect, with the stiffness of *Aristida hystrix* fibre effectively countering compressive stresses, while the energy-absorbing properties of milkweed fibre enhance resistance to tensile cracking. The consistent distribution of fibres and improved bonding at the interface due to the inclusion of peanut shell powder filler lead to enhanced bending performance. A minor decrease in flexural strength to 82 MPa was noted for sample H4. The enhanced fibre content of *Aristida hystrix* contributes to improved stiffness; however, an overabundance of fibre can lead to agglomeration and inadequate wetting of the matrix. The presence of these factors results in interfacial defects that serve as sites for stress concentration during flexural loading, ultimately causing premature failure and diminishing bending strength<sup>68</sup>. The unfilled composite H5 demonstrated a flexural strength of 71 MPa, which is notably less than that of the optimised filler-containing hybrid composite. The lack of peanut shell powder leads to diminished interfacial bonding and increased void content, negatively impacting resistance to bending stresses. This observation highlights the significance of incorporating bio-based fillers to improve interfacial cohesion and flexural performance. The results regarding flexural strength indicate that the combination of fibre hybridisation and the inclusion of peanut shell powder filler notably enhances the bending resistance of epoxy composites. The optimised hybrid composite (H3) exhibits excellent flexural performance, attributed to efficient stress transfer, enhanced interfacial integrity, and well-balanced fibre reinforcement, rendering it appropriate for load-bearing and semi-structural applications<sup>69</sup>.



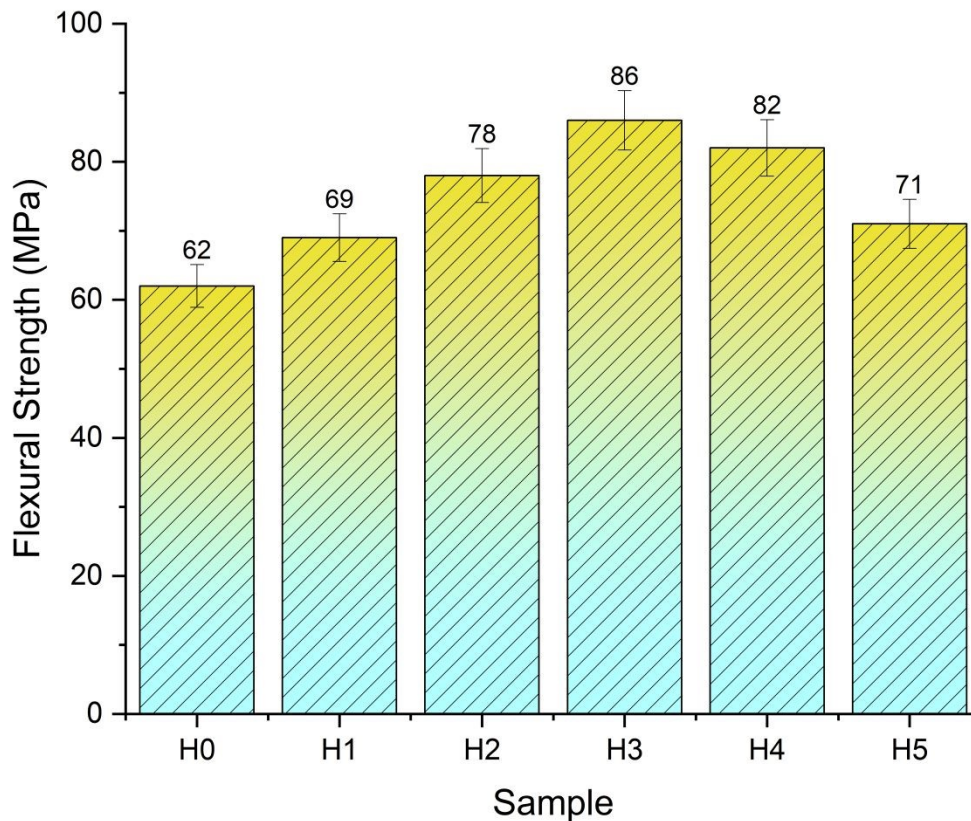


Figure 11 Flexural strength

### 5.5 Flexural Modulus Analysis

The flexural modulus of the milkweed–*Aristida hystrix* fiber reinforced epoxy composites is presented in figure 12. The results show a clear improvement in bending stiffness with increasing fiber hybridization, followed by a slight reduction at higher grass fiber content. The flexural modulus values range from 2.8 to 4.1 GPa, indicating the strong dependence of flexural stiffness on fiber type, dispersion, and fiber–matrix interfacial bonding. Sample H0 exhibited the lowest flexural modulus of 2.8 GPa. The dominance of milkweed fiber in this composite contributes to reduced stiffness due to its hollow lumen structure and relatively low elastic modulus. Under flexural loading, the composite experiences both tensile and compressive stresses, and the limited stiffness of milkweed fiber restricts its ability to resist bending deformation. Although the



presence of peanut shell powder improves matrix compactness, the elastic response is primarily governed by the reinforcing fiber characteristics <sup>70</sup>.

The incorporation of *Aristida hystrix* fiber resulted in a notable increase in flexural modulus. Sample H1 recorded a modulus of 3.2 GPa, reflecting enhanced resistance to bending deformation due to the higher stiffness and cellulose content of the grass fiber. The hybrid fiber system improves stress transfer efficiency and reduces matrix-dominated deformation in the elastic region of the load–deflection curve. Further enhancement is observed in sample H2, which exhibited a flexural modulus of 3.6 GPa. At this composition, the increased proportion of *Aristida hystrix* fiber contributes significantly to stiffness, while the milkweed fiber maintains effective stress distribution across the laminate thickness. The peanut shell powder filler plays a critical role by improving interfacial adhesion and reducing micro-voids, thereby restricting fiber slippage under bending loads <sup>71</sup>. The highest flexural modulus of 4.1 GPa was achieved by sample H3 containing equal proportions of milkweed and *Aristida hystrix* fibers. This balanced hybrid configuration promotes optimal fiber packing, uniform stress distribution, and efficient load transfer within the composite. The synergistic interaction between the stiff grass fiber and the lightweight milkweed fiber, combined with enhanced interfacial integrity provided by the bio-based filler, results in superior resistance to elastic bending deformation.

A slight decrease in flexural modulus to 3.8 GPa was observed for sample H4. Although the higher content of *Aristida hystrix* fiber enhances stiffness, excessive fiber loading can lead to fiber agglomeration, non-uniform dispersion, and insufficient matrix wetting. These interfacial imperfections reduce the effective stiffness contribution of the fibers, limiting further improvement in flexural modulus <sup>72</sup>. The unfilled composite H5 exhibited a relatively low flexural modulus of 2.9 GPa. The absence of peanut shell powder filler results in weaker interfacial bonding and increased void content, which reduce resistance to bending deformation. This comparison highlights the importance of bio-based filler incorporation in enhancing composite stiffness and interfacial efficiency. Overall, the flexural modulus results clearly demonstrate that controlled fiber hybridization combined with peanut shell powder filler incorporation significantly enhances the bending stiffness of epoxy composites. The optimized hybrid composite (H3) exhibits superior flexural rigidity, making it suitable for applications requiring high dimensional stability and resistance to bending loads <sup>73</sup>.



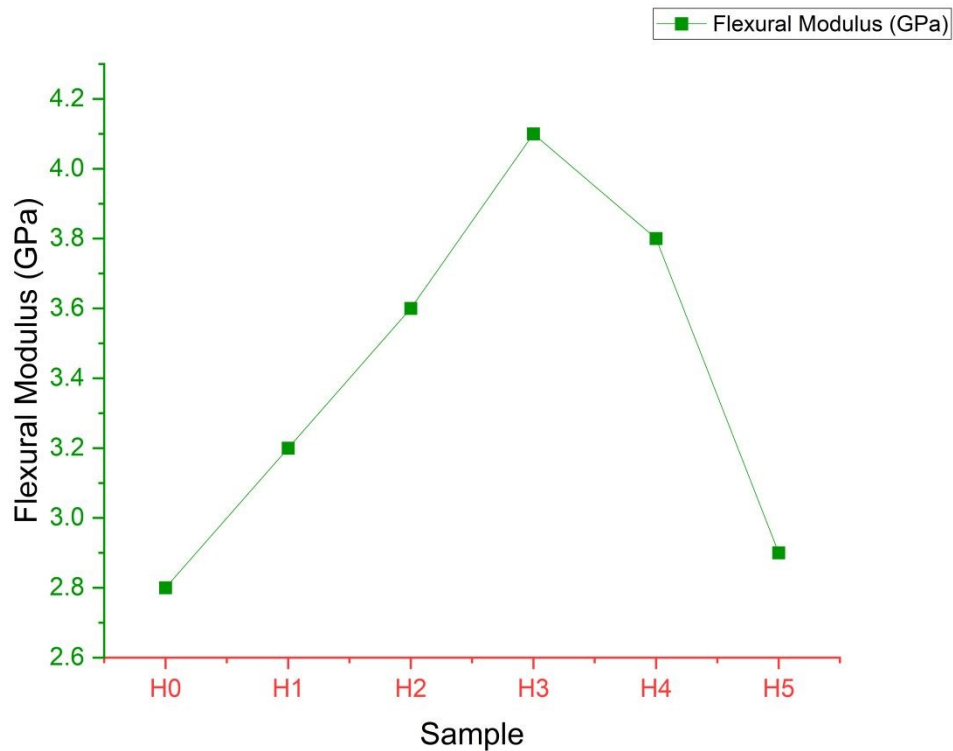


Figure 12 Flexural modulus

### 5.6 Impact Strength Analysis

The impact strength of the milkweed–*Aristida hystrix* fiber reinforced epoxy composites is presented in figure 13. Impact strength is a critical property that reflects the ability of a composite to absorb and dissipate sudden applied energy without catastrophic failure. The results indicate a progressive improvement in impact resistance with fiber hybridization, followed by a slight reduction at higher fiber loading levels. The impact strength values range from 6.8 to 10.2 J, demonstrating the effectiveness of hybrid reinforcement and filler incorporation in enhancing energy absorption capacity. Sample H0 exhibited the lowest impact strength of 6.8 J. This behavior is attributed to the dominance of milkweed fiber, which, despite its lightweight and hollow structure, possesses limited resistance to crack initiation under sudden loading. During impact, the brittle epoxy matrix governs failure, resulting in rapid crack propagation with minimal energy dissipation. The restricted fiber bridging and pull-out mechanisms limit the composite's ability to absorb impact energy effectively<sup>74</sup>. A noticeable improvement in impact



strength was observed for sample H1, which recorded 7.6 J. The introduction of *Aristida hystrix* fiber enhances resistance to crack growth due to its higher tensile strength and stiffness compared to milkweed fiber. The hybrid fiber configuration promotes fiber debonding and controlled pull-out, enabling additional energy dissipation through interfacial friction and matrix deformation during impact. Sample H2 exhibited a further increase in impact strength to 8.9 J. At this composition, the synergistic interaction between milkweed and *Aristida hystrix* fibers becomes more pronounced. The presence of peanut shell powder filler improves fiber–matrix interfacial bonding and reduces micro-voids, thereby delaying crack initiation. Under impact loading, energy is dissipated through multiple mechanisms, including matrix cracking, fiber breakage, fiber pull-out, and crack deflection, resulting in improved toughness<sup>47</sup>. The maximum impact strength of 10.2 J was achieved by sample H3. This composite exhibits an optimal balance between milkweed and *Aristida hystrix* fibers, leading to uniform fiber dispersion and effective stress transfer. The hybrid architecture promotes extensive crack deflection and fiber bridging, significantly increasing the energy required for crack propagation. Additionally, the bio-based filler enhances interfacial cohesion, allowing the composite to sustain higher impact energy before failure. The superior impact performance of H3 correlates well with its enhanced tensile and flexural properties, indicating an optimized microstructural configuration. A marginal decrease in impact strength to 9.4 J was observed for sample H4. Although the higher content of *Aristida hystrix* fiber improves stiffness, excessive fiber loading can result in fiber agglomeration and reduced matrix continuity. These defects act as stress concentrators under impact loading, facilitating crack initiation and limiting further improvement in energy absorption capacity<sup>75</sup>. Sample H5 exhibited an impact strength of 7.9 J, which is significantly lower than the optimized hybrid composite. The absence of peanut shell powder filler weakens interfacial bonding and reduces frictional energy dissipation during fiber pull-out. Consequently, crack propagation occurs more rapidly, leading to reduced impact resistance. Overall, the impact strength results confirm that hybridization of milkweed and *Aristida hystrix* fibers, combined with bio-based filler incorporation, significantly enhances the toughness of epoxy composites. The optimized composite (H3) demonstrates superior energy absorption capability, making it suitable for applications subjected to dynamic and impact loading conditions such as automotive interior panels, protective casings, and lightweight structural components<sup>76</sup>.



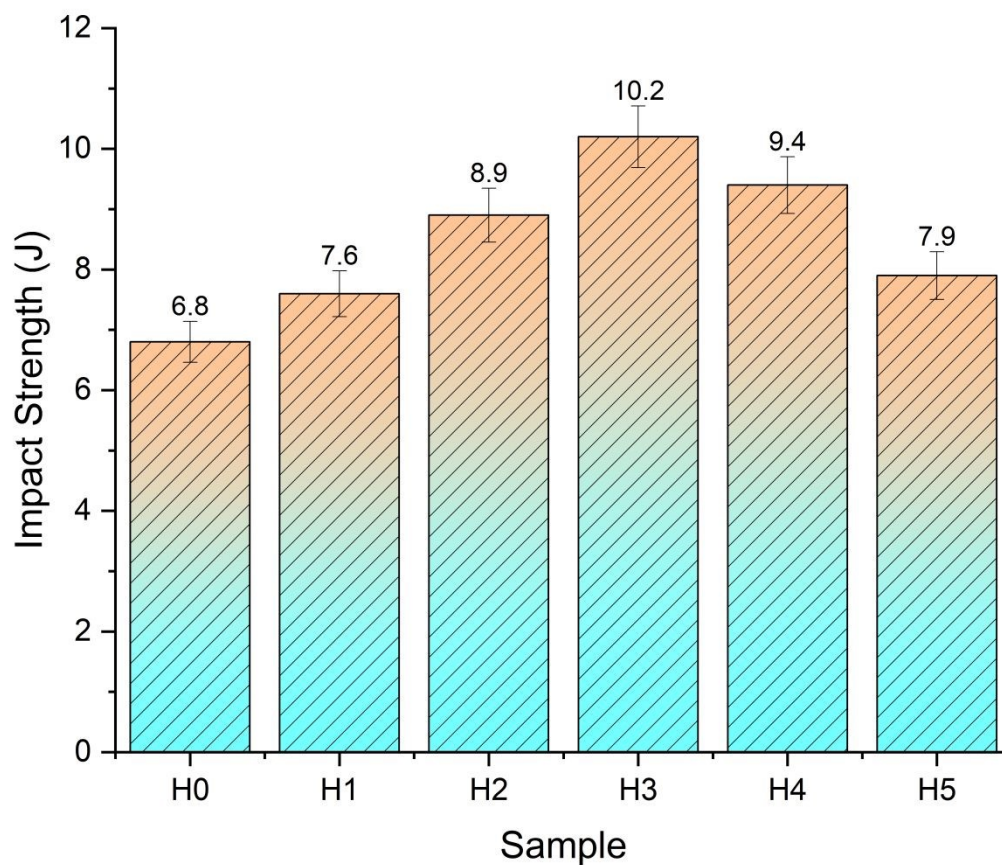


Figure 13 impact strength

### 5.7 Hardness (Shore D) Analysis

The Shore D hardness values of the milkweed–*Aristida hystrix* fiber reinforced epoxy composites are presented in figure 14. Hardness is an important surface property that reflects the resistance of a material to localized plastic deformation and indentation. It is strongly influenced by fiber stiffness, filler content, matrix continuity, and the quality of fiber–matrix interfacial bonding. The hardness values of the developed composites range from 72 to 83 Shore D, indicating a significant variation with fiber hybridization and filler incorporation. Sample H0 exhibited a hardness value of 74 Shore D. The lower hardness of this composite can be attributed to the dominance of milkweed fiber, which has a hollow and comparatively soft structure. The limited stiffness of milkweed fiber reduces resistance to surface indentation, while the epoxy



matrix largely governs the deformation behavior. In addition, weaker interfacial bonding restricts effective load transfer during indentation, resulting in lower hardness<sup>77</sup>. An increase in hardness to 77 Shore D was observed for sample H1. The partial substitution of milkweed fiber with *Aristida hystrix* fiber enhances the composite's resistance to localized deformation due to the higher stiffness and cellulose content of the grass fiber. The improved packing density and better fiber–matrix interaction contribute to increased surface rigidity. Sample H2 recorded a hardness value of 80 Shore D, indicating a substantial improvement in surface resistance. At this composition, the synergistic hybridization of milkweed and *Aristida hystrix* fibers, along with the presence of peanut shell powder filler, promotes effective stress distribution beneath the indenter. The filler particles occupy micro-voids within the matrix and restrict polymer chain mobility, thereby increasing resistance to indentation<sup>78</sup>. The maximum hardness value of 83 Shore D was achieved by sample H3. This behavior is attributed to the optimized hybrid fiber ratio and uniform dispersion of peanut shell powder within the epoxy matrix. The rigid *Aristida hystrix* fibers act as strong load-bearing constituents, while the filler enhances interfacial cohesion and reduces localized matrix deformation. As a result, the composite exhibits superior resistance to surface indentation. A slight reduction in hardness to 81 Shore D was observed for sample H4. Although the higher content of *Aristida hystrix* fiber increases stiffness, excessive fiber loading can lead to fiber agglomeration and reduced resin-rich regions. These microstructural irregularities limit effective stress transfer during indentation, resulting in a marginal decrease in hardness. Sample H5 exhibited the lowest hardness value of 72 Shore D. The absence of peanut shell powder filler and reduced matrix reinforcement weaken the resistance to localized deformation. Poor interfacial bonding and increased matrix-dominated deformation contribute to the observed reduction in hardness<sup>79</sup>. Overall, the hardness results demonstrate that fiber hybridization and bio-based filler incorporation significantly improve the surface mechanical performance of epoxy composites. The optimized hybrid composite (H3) exhibits the highest hardness due to enhanced fiber stiffness, improved interfacial bonding, and reduced matrix deformability. These characteristics make the developed composites suitable for applications requiring improved wear resistance and surface durability<sup>80</sup>.



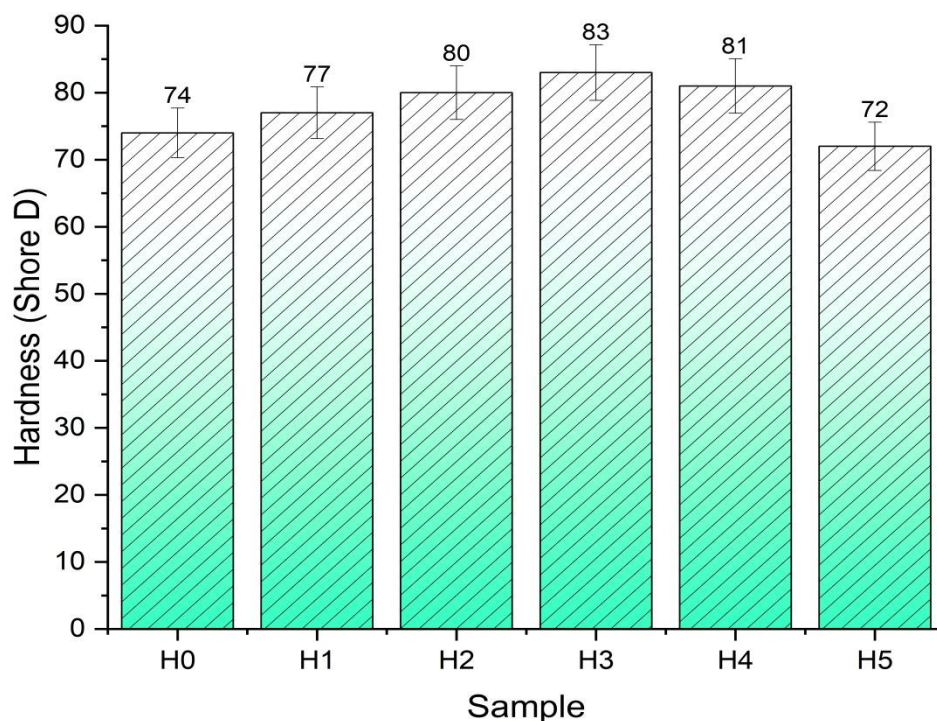


Figure 14 Hardness

### 5.8 Interlaminar Shear Strength (ILSS) Analysis

The interlaminar shear strength (ILSS) values of the milkweed–*Aristida hystrix* fiber-reinforced epoxy composites are illustrated in figure 15. ILSS serves as an essential metric for assessing the adhesion between fibre and matrix, as well as the composite's capability to transmit shear stresses at the interfaces. Changes in ILSS are directly influenced by the hybridisation of fibres, the distribution of fillers, and the quality of interfacial bonding within the composite system. Sample H0 exhibited an ILSS value of 7.8 MPa. The relatively lower ILSS is primarily attributed to the dominance of milkweed fiber, which possesses a hollow structure and smooth surface morphology. These characteristics reduce mechanical interlocking with the epoxy matrix and limit shear stress transfer at the interface. In addition, the presence of micro-voids and weak bonding zones contributes to premature interfacial debonding under shear loading<sup>81</sup>. An increase in ILSS to 8.9 MPa was observed for sample H1. The introduction of *Aristida hystrix* fiber enhances interfacial adhesion due to its higher cellulose content and rougher surface texture,



which promotes better mechanical interlocking with the epoxy resin. The synergistic interaction between the two fibers improves load-sharing mechanisms under interlaminar shear stress. Sample H2 recorded a significantly higher ILSS value of 10.4 MPa. At this composition, improved fiber dispersion and uniform peanut shell powder distribution enhance the interfacial region. The filler particles act as stress-transfer bridges between the fibers and matrix, reducing stress concentration and delaying interfacial crack initiation. This results in improved resistance to shear-induced delamination. The maximum ILSS of 12.1 MPa was achieved by sample H3, indicating optimal interfacial bonding. The balanced hybrid fiber ratio combined with effective filler incorporation leads to a dense and well-integrated microstructure. The peanut shell powder fills interfacial gaps and restricts crack propagation, while *Aristida hystrix* fibers provide enhanced shear load-bearing capability. SEM observations typically reveal minimal fiber pull-out and cohesive matrix failure for such optimized composites, supporting the observed ILSS improvement. A slight reduction in ILSS to 11.2 MPa was noted for sample H4. Although higher *Aristida hystrix* fiber content increases stiffness, excessive fiber loading can result in agglomeration and incomplete wetting by the resin. These microstructural defects weaken the interlaminar region, leading to a marginal decline in shear strength. Sample H5 exhibited the lowest ILSS value of 7.1 MPa. The absence of peanut shell powder filler reduces interfacial reinforcement, while higher overall fiber content leads to insufficient resin availability for effective bonding. Poor fiber–matrix adhesion and increased interfacial voids contribute to early delamination under shear loading<sup>82</sup>. Overall, the ILSS results clearly demonstrate that fiber hybridization and bio-based filler incorporation significantly enhance interfacial strength in epoxy composites. The optimized composite (H3) shows superior resistance to interlaminar shear failure due to improved bonding, effective stress transfer, and reduced interfacial defects<sup>76,83</sup>. These findings highlight the effectiveness of combining rare natural fibers with agricultural waste fillers to develop high-performance and sustainable composite materials.



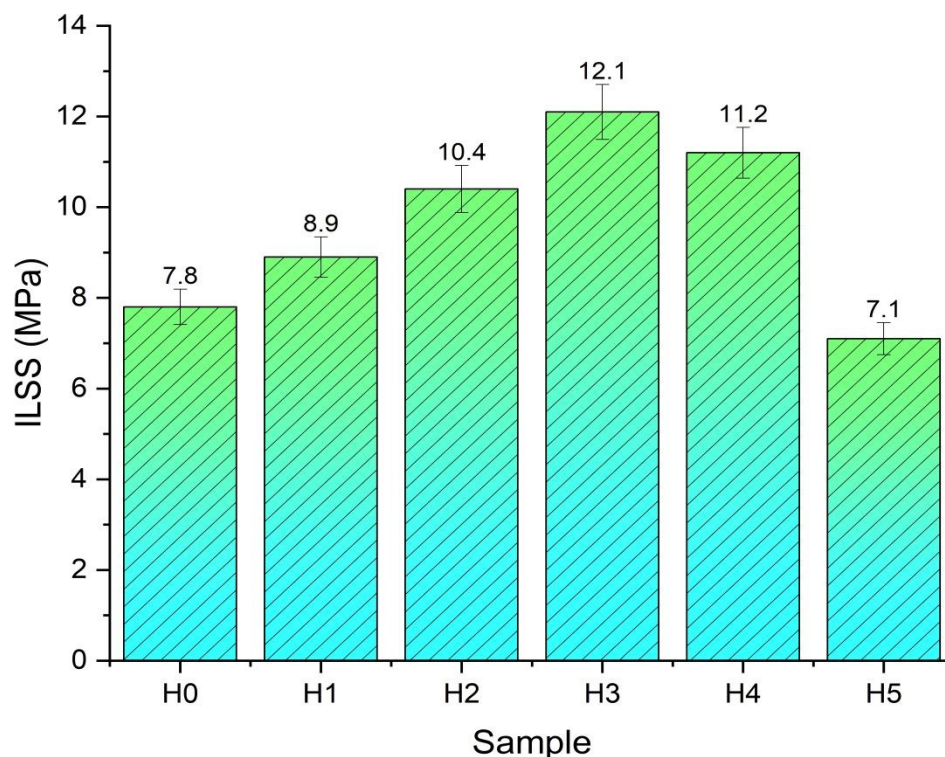


Figure 15 ILSS of Samples

### 5.9 Scanning Electron Microscopy (SEM) Analysis

Scanning electron microscopy (SEM) was employed to examine the tensile fracture surfaces of the milkweed–*Aristida hystrix* fiber reinforced epoxy composites in order to correlate microstructural features with the observed mechanical performance as shown in figure 16. The SEM analysis provides insight into fiber–matrix interfacial bonding, fiber dispersion, filler distribution, and dominant failure mechanisms across different hybrid compositions <sup>84</sup>.

The fracture surface of sample H0 (a) reveals a relatively rough and heterogeneous morphology characterized by noticeable fiber pull-out, interfacial gaps, and micro-voids. The hollow structure of milkweed fibers and their smooth surface morphology result in weak mechanical interlocking with the epoxy matrix. These features promote premature interfacial debonding and matrix



cracking, which explains the lower tensile strength, modulus, and ILSS observed for this composite <sup>83</sup>.

Sample H1 (b) exhibits improved interfacial characteristics compared to H0. SEM micrographs show reduced fiber pull-out and better fiber embedment within the epoxy matrix. The introduction of *Aristida hystrix* fiber enhances surface roughness and promotes mechanical interlocking, leading to more effective stress transfer. However, localized matrix cracks and limited voids are still visible, indicating partial improvement in interfacial bonding.

In sample H2 (c), the fracture surface appears more compact and uniform. The fibers are well dispersed and firmly anchored within the matrix, with fewer interfacial voids. The peanut shell powder filler is observed to be uniformly distributed, occupying micro-gaps between fibers and the matrix. This microstructural refinement contributes to enhanced tensile and flexural properties, as well as improved interlaminar shear strength <sup>85</sup>.

Sample H3 (d) demonstrates the most refined and homogeneous fracture morphology among all compositions. SEM images show strong fiber–matrix adhesion, minimal fiber pull-out, and extensive matrix deformation surrounding the fibers. The filler particles are well integrated within the matrix, acting as crack-arresting sites and promoting crack deflection. The dominant failure mode shifts from interfacial debonding to cohesive matrix fracture and fiber breakage, which is consistent with the superior mechanical performance and higher strain-to-failure observed for this composite <sup>86</sup>.

In sample H4 (e), although good fiber–matrix bonding is still evident, regions of fiber agglomeration and resin-starved zones are occasionally observed. These microstructural irregularities introduce localized stress concentrations, leading to reduced resistance against crack propagation. As a result, a slight decline in mechanical properties and ILSS is observed compared to H3.

Sample H5 (f) exhibits poor interfacial characteristics, with extensive fiber pull-out, voids, and matrix cracking. The absence of peanut shell powder filler limits interfacial reinforcement, and insufficient resin wetting at higher fiber content further weakens the composite structure. The



fracture surface morphology confirms interfacial failure as the dominant mechanism, correlating with the lower mechanical and interlaminar properties of this sample.

Overall, SEM analysis clearly demonstrates that optimized fiber hybridization and bio-based filler incorporation significantly enhance fiber–matrix interfacial bonding and microstructural integrity<sup>87</sup>. The superior morphology of sample H3 validates its enhanced mechanical performance and confirms the strong structure–property relationship in the developed sustainable hybrid composites.

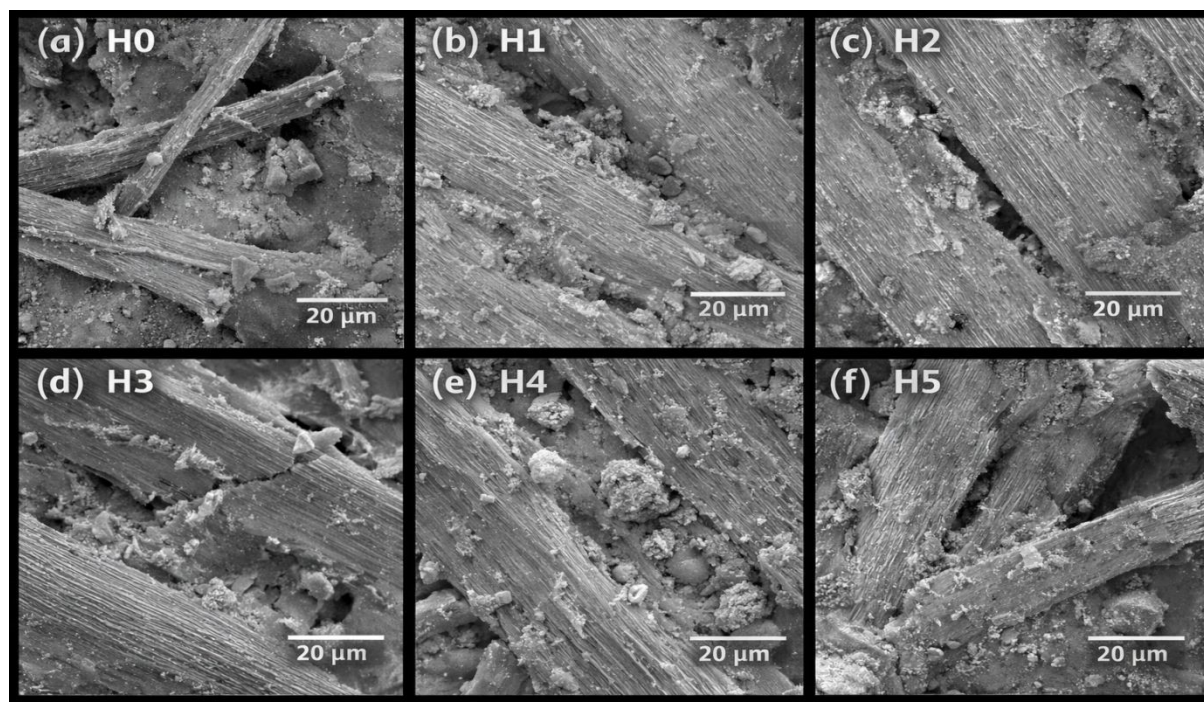


Figure 16 SEM Images of all samples

## 6.0 Conclusions

The present study systematically investigated the effect of fiber hybridization and bio-based filler incorporation on the mechanical, interfacial, and microstructural performance of milkweed–*Aristida hystrix* fiber-reinforced epoxy composites. Based on the experimental results and detailed analyses, the following conclusions are drawn:



1. **Effect of fiber hybridization:** Hybridization of milkweed fiber with the lesser-explored *Aristida hystrix* fiber significantly enhanced the tensile, flexural, impact, hardness, and interlaminar shear properties of the epoxy composites. This improvement is attributed to the higher stiffness, rough surface morphology, and superior cellulose content of *Aristida hystrix* fiber, which effectively complements the lightweight and energy-absorbing characteristics of milkweed fiber.
2. **Role of peanut shell powder filler:** The incorporation of peanut shell powder acted as an effective bio-based micro-reinforcement by improving fiber–matrix interfacial adhesion and reducing micro-voids. The filler enhanced stress transfer efficiency, restricted crack propagation, and contributed to increased tensile modulus, flexural modulus, hardness, and interlaminar shear strength (ILSS) compared to the filler-free composite.
3. **Mechanical performance optimization:** Among all compositions, sample H3 (15 wt% milkweed fiber, 15 wt% *Aristida hystrix* fiber, and 10 wt% peanut shell powder) exhibited the best overall mechanical performance, with a tensile strength of 61 MPa, flexural strength of 86 MPa, impact strength of 10.2 J, hardness of 83 Shore D, and an ILSS of 12.1 MPa, along with improved tensile and flexural moduli. These results confirm the presence of an optimal hybrid fiber ratio that effectively balances stiffness, strength, and toughness.
4. **Stress–strain behavior:** The optimized hybrid composite demonstrated enhanced ductility and damage tolerance, sustaining higher stress over a broader strain range. The gradual post-peak stress reduction observed in the hybrid composites indicates controlled failure mechanisms, such as fiber bridging and crack deflection, rather than abrupt brittle fracture.
5. **Microstructural correlation:** SEM analysis revealed that the improved mechanical performance is closely associated with enhanced microstructural integrity. Sample H3 showed strong fiber–matrix adhesion, minimal fiber pull-out, uniform filler dispersion, and cohesive matrix failure, which collectively validate the observed improvements in mechanical and interlaminar properties.
6. **Sustainability and application potential:** The use of locally sourced natural fibers and agricultural waste fillers highlights the sustainability of the developed composites. The superior performance of the optimized hybrid system makes it a promising candidate for



lightweight structural and semi-structural applications, particularly in eco-friendly engineering sectors such as automotive interior components, panels, and low-load structural parts.

Overall, this study demonstrates that the strategic combination of underutilized natural fibers and bio-based fillers is an effective approach for developing high-performance, sustainable epoxy composites, while also promoting the valorization of agricultural waste materials.

### **CRedit authorship contribution statement**

**Manickaraj Karuppusamy**: Conceptualization, Methodology, Supervision, Writing – Review & Editing; **Sivasubramanian Palanisamy**: Data Curation, Formal Analysis, Writing – Original Draft; **Silambarasan Balakrishnamoorthi**: Investigation, Validation, Visualization; **Ashok Raj Rajendran**: Software, Formal Analysis, Data Curation; **Subbiah Parvathy Velmurugan**: Investigation, Resources, Validation; **Kumar Sureshkumar**: Methodology, Supervision, Writing – Review & Editing; **Syed Kashif Ali**: Software, Visualization, Data Curation; **Subramanian Lakshmi Sankar**: Formal Analysis, Validation, Writing – Review & Editing; **Karthikayan Sundararajan**: Investigation, Resources, Project Administration; **Aravindhyan Alagarsamy**: Data Curation, Visualization, Writing – Original Draft; **Mezigebe Belay**: Supervision, Conceptualization, Funding Acquisition, Writing – Review & Editing.

### **Declaration of competing interest**

The authors declare that they have no known competing financial interests or personal relationships that could have appeared to influence the work reported in this paper.

### **Data availability**

Data will be made available on request



## Reference

- 1 R. Mandala, G. Hegde, D. Kodali and V. R. Kode, *Journal of Composites Science*, 2023, **7**, 307.
- 2 M.-B. Coltelli, L. Aliotta, V. Gigante and A. Lazzeri, in *Nanomaterials in Agroforestry Systems*, Springer, 2025, pp. 67–98.
- 3 K. Manickaraj, R. Ramamoorthi, R. Karuppasamy, K. R. Sakthivel and B. Vijayaprakash, *Evolutionary Manufacturing, Design and Operational Practices for Resource and Environmental Sustainability*, 2024, 135–141.
- 4 N. B. Arzumanova, *New Mater Comp Appl*, 2021, **5**, 19–44.
- 5 N. Sienkiewicz, M. Dominic and J. Parameswaranpillai, *Polymers*, 2022, **14**, 265.
- 6 O. I. Oladele, A. D. Akinwekomi, J. G. Akinseye, S. O. Falana and S. R. Oke, *Journal of Composite Materials*, 2024, **58**, 2597–2622.
- 7 R. Reh, L. Kristak and P. Antov, *Materials*, 2022, **15**, 8651.
- 8 M. Jawaid, M. T. Paridah and N. Saba, *Lignocellulosic fibre and biomass-based composite materials: processing, properties and applications*, Woodhead Publishing, 2017.
- 9 P. Krishnasamy and G. Rajamurugan, *Sustainable Smart Composites: Technology, and Applications*, 2025, 1.
- 10 V. Guna, M. Ilangovan, M. H. Rather, B. V Giridharan, B. Prajwal, K. V. Krishna, K. Venkatesh and N. Reddy, *Journal of Building engineering*, 2020, **27**, 100991.
- 11 M. Ramesh, L. N. Rajeshkumar, N. Srinivasan, D. V. Kumar and D. Balaji, *e-Polymers*, 2022, **22**, 898–916.
- 12 M. J. Mochane, T. C. Mokhena, T. H. Mokhothu, A. Mtibe, E. R. Sadiku, S. S. Ray, I. D. Ibrahim and O. O. Daramola, .
- 13 M. Ramesh, M. Tamil Selvan, L. Rajeshkumar, C. Deepa and A. Ahmad, *Journal of Natural Fibers*, 2022, **19**, 13776–13789.
- 14 S. Gokul, T. Ramakrishnan, K. Manickaraj, P. Devadharshan, M. K. Mathew and T. V.



- Prabhu, in *AIP Conference Proceedings*, AIP Publishing, 2024, vol. 3221.
- 15 M. A. Al Mamun, H. Aftab, M. H. Hasan, M. A. Khan and G. M. S. Rahman, *ChemistrySelect*, 2025, **10**, e02119.
- 16 S. Sanchez-Diaz, C. Ouellet, S. Elkoun and M. Robert, *Polymer Composites*, 2023, **44**, 2723–2734.
- 17 A. Nourbakhsh, A. Ashori and M. Kouhpayehzadeh, *Journal of reinforced plastics and composites*, 2009, **28**, 2143–2149.
- 18 T. Karthik and R. Murugan, in *Sustainable Fibres for Fashion Industry: Volume 2*, Springer, 2016, pp. 111–146.
- 19 M. Gurusamy, R. Thirumalaisamy, M. Karuppusamy and G. Sivanantham, *Journal of Polymer Research*, 2025, **32**, 1–26.
- 20 M. Sayanjali Jasbi, H. Hasani, A. Zadhoush and S. Safi, *The Journal of The Textile Institute*, 2018, **109**, 24–31.
- 21 P. Ovlaque, M. Foruzanmehr, S. Elkoun and M. Robert, *Composite Interfaces*, 2020, **27**, 495–513.
- 22 S. Sanchez-Diaz, C. Ouellet, S. Elkoun and M. Robert, *Journal of Natural Fibers*, 2023, **20**, 2174630.
- 23 L. Jamalirad, H. Aminian and S. Hedjazi, *Journal of Natural Fibers*, 2019, **16**, 77–87.
- 24 A. I. B. Idriss, C. Mei Yang, J. Li, A. A. A. Abdelmagid, H. Zhang and E. A. I. Ahmed, *Rapid Prototyping Journal*, 2025, **31**, 2133–2149.
- 25 Y. Wang, Y. Chen, L. Wang, Y. Mo, X. Lin, S. Gao and M. Chen, *Process Biochemistry*, 2025, **154**, 22–34.
- 26 F. Faraji, M. Abdalqadir, S. Rezaei-Gomari, J. A. Ali, B. S. Mahmood and D. Hughes, *Chemical Papers*, 2025, **79**, 4213–4228.
- 27 A. Sabziparvar and M. R. Foruzanmehr, *Case Studies in Construction Materials*, 2024, **21**, e03946.
- 28 M. Mula, R. N. Tekbas, F. Cengiz, I. O. Yüksek and A. Gurarslan, *ACS Sustainable Chemistry & Engineering*, 2023, **11**, 12523–12531.



- 29 D. Lupescu, P. Cousin, M. Robert and S. Elkoun, *Materials*, 2025, **18**, 618.
- 30 D. Lupescu, M. Robert and S. Elkoun, *Materials*, 2025, **18**, 3821.
- 31 P. Khanna and P. L. Ramkumar, *Journal of Thermoplastic Composite Materials*, 2026, **39**, 941–962.
- 32 P. Ovlaque, M. Bayart, S. Elkoun and M. Robert, *Composite Interfaces*, 2022, **29**, 215–235.
- 33 E. Kalayci, O. Avinc and K. B. Turkoglu, in *Sustainable approaches in textiles and fashion: Fibres, raw materials and product development*, Springer, 2022, pp. 1–21.
- 34 D. Lupescu, M. Robert, S. Sanchez-Diaz and S. Elkoun, *Textiles*, 2025, **5**, 5.
- 35 J. Wang, K. Dong, Z. Sun, L. Kong, B. Tang, S. Wu, X. Huang and F. Guo, *Journal of Analytical and Applied Pyrolysis*, 2025, **189**, 107110.
- 36 S. Sanchez-Diaz, 2023.
- 37 A. Sabziparvar, D. Taleponga and M. R. Foruzanmehr, in *Interdisciplinary Symposium on Smart & Sustainable Infrastructures*, Springer, 2023, pp. 159–171.
- 38 S. B. Boppana, K. Palani Kumar, A. Ponshanmugakumar and S. Dayanand, *Bio-Fiber Reinforced Composite Materials: Mechanical, Thermal and Tribological Properties*, 2022, 51–73.
- 39 R. E. Harry-O'kuru, A. Mohamed, S. H. Gordon and J. Xu, *Journal of agricultural and food chemistry*, 2012, **60**, 1688–1694.
- 40 G. Godwin, G. A. Miraculas, S. J. Arul and S. K., *Journal of Mechanical Science and Technology*, 2026, 1–14.
- 41 S. Soulié, I. Bilem, P. Chevallier, S. Elkoun, M. Robert, N. Naudé and G. Laroche, *International Journal of Polymeric Materials and Polymeric Biomaterials*, 2020, **69**, 872–883.
- 42 N. Tarabi, H. Mousazadeh, A. Jafari and J. Taghizadeh-Tameh, *Engineering in Agriculture, Environment and Food*, 2015, **8**, 88–94.
- 43 D. Lupescu, M. Robert and S. Elkoun, *Fibers*, 2025, **13**, 4.
- 44 K. Z. Alzarieni, A. R. Bani Amer and H. I. Kenttämaa, *Journal of Natural Fibers*, 2025,



- 22, 2546019.
- 45 P. Khanna and P. L. Ramkumar, *Journal of Macromolecular Science, Part B*, 2026, **65**, 127–149.
- 46 N. V Chithra, R. Karuppasamy, K. Manickaraj and T. Ramakrishnan, *J. Environ. Nanotechnol*, 2024, **13**, 65–79.
- 47 K. Manickaraj, A. Karthik, S. Palanisamy, M. Jayamani, S. K. Ali, S. L. Sankar and S. A. Al-Farraj, *BioResources*, 2025, **20**, 1998–2025.
- 48 K. Hariprasad, K. Ravichandran, V. Jayaseelan and T. Muthuramalingam, *Journal of Materials Research and Technology*, 2020, **9**, 14029–14035.
- 49 N. H. Alrasheedi, P. Sivasubramanian, M. Karuppusamy, B. Haldar and T. K. Durairaj, *BioResources*, 2026, **21**, 459–481.
- 50 P. Nguyen-Tri, P. Carrière, A. Duong and S. Nanda, *ACS omega*, 2020, **5**, 22430–22439.
- 51 M. Karuppusamy, S. Kalidas, S. Palanisamy, K. Nataraj, R. K. Nandagopal, R. Natarajan, A. Samraj, N. Ayrilmis, S. K. Sahu and J. Giri, *BioResources*.
- 52 M. J. Raghu and G. Goud, *Applied Mechanics and Materials*, 2019, **895**, 45–51.
- 53 S. C. Venkateshappa, S. Y. Jayadevappa and P. K. W. Puttiah, *Advances in Polymer Technology*, 2012, **31**, 319–330.
- 54 Y. Liu, J. Xie, N. Wu, L. Wang, Y. Ma and J. Tong, *Tribology International*, 2019, **131**, 398–405.
- 55 K. Manickaraj, R. Thirumalaisamy, S. Palanisamy, N. Ayrilmis, E. E. S. Massoud, M. Palaniappan and S. L. Sankar, *Annals of the New York Academy of Sciences*.
- 56 L. Jamalirad and S. B. Hosseini, *Iranian Journal of Wood and Paper Industries*, 2019, **10**, 115–124.
- 57 S. Boopathi, M. Sureshkumar, M. Jeyakumar, R. S. Kumar and R. Subbiah, in *Materials Science Forum*, Trans Tech Publ, 2022, vol. 1075, pp. 115–124.
- 58 S. Kaliappan, L. Natrayan, P. V. A. Kumar and A. Raturi, *Biomass Conversion and Biorefinery*, 2024, **14**, 24061–24068.
- 59 S. D. S. Koppaarthi, .



- 60 A. K. Ramasamy, S. Selvaraj, A. Murugan and S. K. Rathinasamy, *Proceedings of the Institution of Mechanical Engineers, Part C: Journal of Mechanical Engineering Science*, 2024, **238**, 5087–5096.
- 61 K. Kalauni and S. J. Pawar, *Iranian Polymer Journal*, 2025, **34**, 1073–1083.
- 62 G. Krishnadas, R. Karuppasamy, S. Selvam and K. Manickaraj, *MATERIA-RIO DE JANEIRO*.
- 63 G. Ravichandran, K. Ramasamy, K. Manickaraj, S. Kalidas, M. Jayamani, K. Mausam, S. Palanisamy, Q. Ma and S. A. Al-Farraj, *BioResources*, 2025, **20**, 8674–8694.
- 64 J. Nanthakumar, Y. Palanisamy, S. Palanisamy, M. Karuppusamy, R. Raja, M. Abbas, A. Alagarsamy and M. Z. Rahman, *RSC Advances*, 2025, **15**, 39305–39313.
- 65 G. Ramesh, K. Subramanian, S. Sathiyamurthy and M. Prakash, *Journal of Natural Fibers*, 2022, **19**, 3668–3680.
- 66 K. R. Sumesh, A. Ajithram, S. Palanisamy and V. Kavimani, *Biomass Conversion and Biorefinery*, 2023, 1–12.
- 67 R. Jayaraman, M. Viknesh and R. Girimurugan, *Materials Today: Proceedings*, 2023, **74**, 636–641.
- 68 P. Ovlaque, M. Bayart, S. Elkoun and M. Robert, *CAMX 2019*.
- 69 C. Uthemann and T. Gries, *Materials*, 2025, **18**, 4469.
- 70 P. Krishnasamy, G. Rajamurugan, S. Aravindraj and P. E. Sudhagar, *Journal of Natural Fibers*, 2022, **19**, 2885–2901.
- 71 M. H. Mazaherifar, H. Z. Hosseinabadi, C. Coşoreanu, C. Cerbu, M. C. Timar and S. V. Georgescu, *Forests*, 2022, **13**, 2098.
- 72 R. J. M. Wolfs, F. P. Bos and T. A. M. Salet, *Cement and Concrete Research*, 2018, **106**, 103–116.
- 73 P. V Badyankal, T. S. Manjunatha, P. S. S. Gouda, M. P. BH and C. S. Srinivasa, *Engineering Research Express*, 2024, **6**, 15507.
- 74 M. N. Prabhakar, A. U. R. Shah, K. C. Rao and J.-I. Song, *Fibers and Polymers*, 2015, **16**, 1119–1124.



- 75 N. Arasu and K. Manickaraj, *Zastita Materijala*.
- 76 N. F. Zaaba, H. Ismail and M. Jaafar, *BioResources*, 2013, **8**, 5826–5841.
- 77 M. A. Nkansah, M. Donkoh, O. Akoto and J. H. Ephraim, .
- 78 P. Pączkowski, A. Puszka and B. Gawdzik, *Polymers*, 2021, **13**, 3690.
- 79 N. E. Ikladios, N. Shukry, S. F. El-Kalyoubi, J. N. Asaad, S. H. Mansour, S. Y. Tawfik and R. E. Abou-Zeid, *Proceedings of the Institution of Mechanical Engineers, Part L: Journal of Materials: Design and Applications*, 2019, **233**, 955–964.
- 80 T. Ramakrishnan, K. Manickaraj, S. P. Prithiv, S. L. Aditya, N. Rajanarayanan and S. Gopalsamy, in *AIP Conference Proceedings*, AIP Publishing, 2024, vol. 3221.
- 81 B. Wang, J. Shen, S. Li and W. Wang, *Materials*, 2023, **16**, 6618.
- 82 M. Wu, Q. Guo and G. Fu, *Powder technology*, 2013, **247**, 188–196.
- 83 N. F. Zaaba, H. Ismail and M. Mariatti, *Procedia Chemistry*, 2016, **19**, 763–769.
- 84 X. Liu, X. Dong, S. Chang, X. Xu, J. Li and H. Pu, *Environmental Geochemistry and Health*, 2023, **45**, 9599–9619.
- 85 K. Manickaraj, S. Palanisamy, C. Manivel and N. R. Kumar, in *Biomimetic and Bioinspired Materials*, CRC Press, 2025, pp. 3–21.
- 86 P. Pandiarajan, P. G. Baskaran, S. Palanisamy, M. Karuppusamy, K. Marimuthu, A. Rajan, M. I. Almansour, Q. Ma and S. A. Al-Farraj, *BioResources*, 2025, **20**, 9257–9281.
- 87 K. Manickaraj, T. Nithyanandhan, K. Sathish, R. Karuppasamy and B. Sachuthananthan, in *2024 10th International Conference on Advanced Computing and Communication Systems (ICACCS)*, IEEE, 2024, vol. 1, pp. 2373–2378.



## Data Availability Statement

View Article Online  
DOI: 10.1039/D6SU00165C

Data are available on request from the authors.

